

Optimized Opioid-Neurotensin Multitarget Peptides: From Design to Structure–Activity Relationship Studies

Simon Gonzalez, Maria Dumitrascuta, Emilie Eiselt, Stevany Louis, Linda Kunze, Annalisa Blasiol, Mélanie Vivancos, Santo Previti, Elke Dewolf, Charlotte Martin, Dirk Tourwé, Florine Cavalier, Louis Gendron, Philippe Sarret,* Mariana Spetea,* and Steven Ballet*

Cite This: *J. Med. Chem.* 2020, 63, 12929–12941

Read Online

ACCESS |



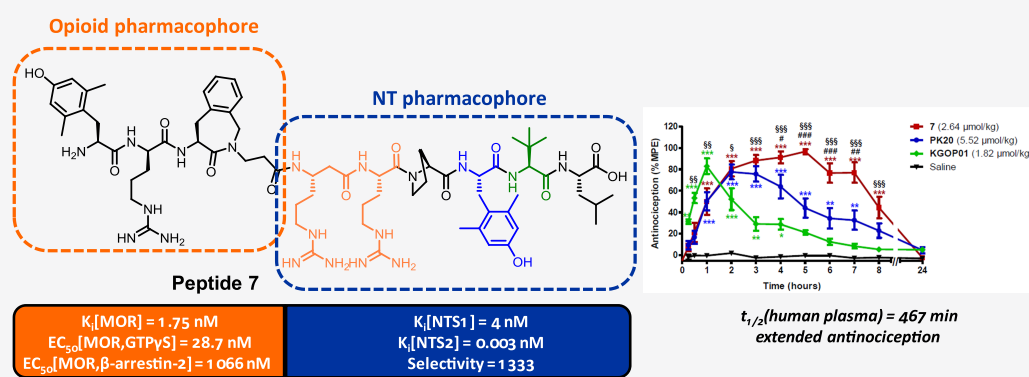
Metrics & More



Article Recommendations



Supporting Information



ABSTRACT: Fusion of nonopioid pharmacophores, such as neurotensin, with opioid ligands represents an attractive approach for pain treatment. Herein, the μ - δ -opioid agonist tetrapeptide H-Dmt-D-Arg-Aba- β -Ala-NH₂ (KGOP01) was fused to NT(8-13) analogues. Since the NTS1 receptor has been linked to adverse effects, selective MOR-NTS2 ligands are preferred. Modifications were introduced within the native NT sequence, particularly a β^3 -homo amino acid in position 8 and Tyr¹¹ substitutions. Combination of β^3 hArg and Dmt led to peptide 7, a MOR agonist, showing the highest NTS2 affinity described to date ($K_i = 3$ pM) and good NTS1 affinity ($K_i = 4$ nM), providing a >1300-fold NTS2 selectivity. The (6-OH)Tic-containing analogue 9 also exhibited high NTS2 affinity ($K_i = 1.7$ nM), with low NTS1 affinity ($K_i = 4.7$ μ M), resulting in an excellent NTS2 selectivity (>2700). In mice, hybrid 7 produced significant and prolonged antinociception (up to 8 h), as compared to the KGOP01 opioid parent compound.

INTRODUCTION

Pain remains a major global health concern affecting the worldwide population. Moderate to severe pain is nowadays treated by opioid analgesics such as morphine, oxycodone, and fentanyl that activate the μ -opioid receptor (MOR). Nonetheless, opioid drugs are causing several adverse effects including constipation, respiratory depression, sedation, and nausea, and their chronic administration is associated with dependence liability and analgesic tolerance.¹ Consequently, the treatment of chronic pain by opioids remains troublesome. In addition, the growing number of overdoses and deaths caused by misuse of and addiction to opioids is a public health concern.² To overcome the aforementioned opioid-related limitations and to combat the current opioid crisis, several strategies have emerged during the past decades. These include the development of drugs with opioid-independent actions (e.g., neurotensin, neuropeptide FF, cannabinoids, melanocortin, and substance P analogues),³ the design of chimeric chemical entities showing two pharmacophores involved in pain regulation/signaling, most commonly an opioid coupled to a

nonopioid part,⁴ and generation of G protein-biased opioid agonists.⁵

As one of the nonopioid pharmacophores, neurotensin (NT) receptor ligands can be considered. NT is a natural neuropeptide composed of 13 amino acids, isolated by Carraway and Leeman in 1973 from bovine hypothalamus and later on from the bovine small intestine (Figure 1).⁶ This neuropeptide is the endogenous ligand of three receptors: NTS1 and NTS2 belonging to the GPCR superfamily, whereas NTS3 also called sortilin is a single transmembrane domain receptor.⁷ Over the past decades, NT and its receptors were shown to be responsible for or involved in various biological effects, such as food intake regulation, modulation of pituitary

Received: August 5, 2020

Published: September 9, 2020



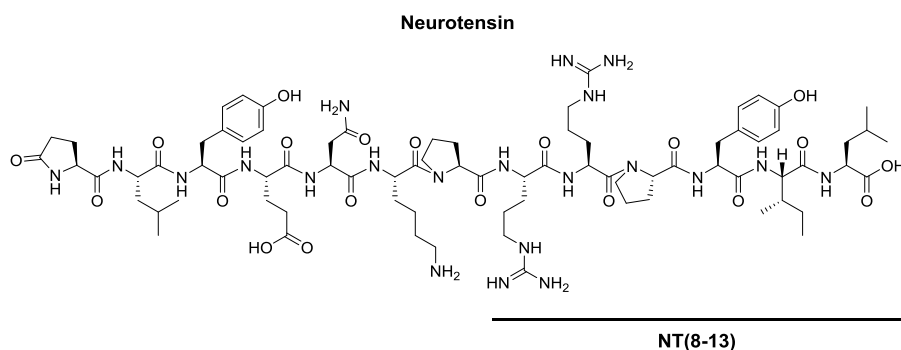


Figure 1. Chemical structure of neurotensin and NT(8-13).

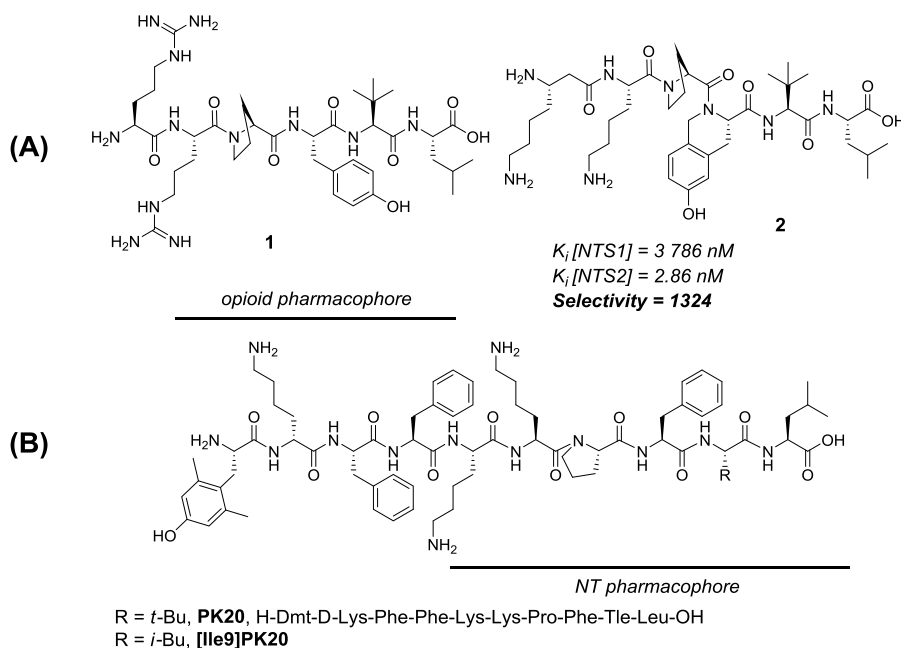


Figure 2. (A) Previously described NT(8-13) analogues. (B) Chemical structure of the OP-NT chimeric peptide, **PK20**.

hormone release, and opioid-independent antinociception.⁷ The discovery that the C-terminus hexapeptide, namely, NT(8-13) (H-Arg-Arg-Pro-Tyr-Ile-Leu-OH), could serve as NT's minimal active sequence for receptor binding and activation led to increasing interest for NT analogues with improved pharmacokinetic features (Figure 1).⁸

Although generally characterized by a rapid proteolytic degradation and poor blood–brain barrier (BBB) permeation, NT(8-13) analogues with potent antinociceptive activity have been described, particularly in acute, tonic, and neuropathic pain models.⁹ Among the NT receptors, NTS1 and NTS2 were extensively associated with NT-induced analgesia, exerting naloxone and naltrexone-independent analgesic responses.¹⁰ While NTS1 was initially identified as the main target for antinociception and several potent ligands were discovered, the focus gradually shifted to NTS2 to prevent NTS1-related physiological effects, such as hypotension and hypothermia.^{9f} Hence, NTS2-selective, but also more generally NTS1/2, agonists represent a promising alternative to opioid analgesics for the treatment of chronic pain. As recently reported by our groups, modifications within the NT native sequence such as Tle¹², Dmt¹¹, or (6-OH)Tic¹¹ have a significant effect on NTS2/NTS1 selectivity and plasma stability.¹¹ Substitution of the two native basic residues Arg⁸

and Arg⁹ by β^3 hLys⁸ and Lys⁹ improves even more both selectivity and stability, as exemplified by peptide **2** (Figure 2A; NTS2/NTS1 selectivity > 1300; $t_{1/2}$ > 24 h).¹¹

Ever since Morphy and Rankovich introduced the concept of designed multiple ligands (DMLs) or multitarget drugs, the field of medicinal chemistry has seen an extensive effort for developing more efficient and safer treatments for human diseases using such an approach.¹² Because pain is a highly complex physiological and psychological phenomenon involving different molecular targets, the use of multitarget compounds for effective analgesia has been shown to be a successful strategy. This is illustrated by several examples, particularly applying the fusion of opioid (OP) with nonopioid pharmacophores, such as substance P, NT, cholecystokinin, cannabinoids, melanocortin ligands, and their respective analogues.⁴ More recently, our groups developed a new OP-neuropeptide FF ligand showing agonism at the MOR and antagonism at the NPFF receptors, exhibiting effective and potent analgesia in mouse models of acute and inflammatory pain as well as reduced opioid-induced adverse effects, including respiratory depression, hyperalgesia, tolerance, and withdrawal syndrome.¹³ Several studies have also highlighted the potency of combining opioid and NT pharmacophores in order to obtain superior analgesia and reduced unwanted side

effects.¹⁴ Accordingly, Eiselt *et al.* recently described that the coadministration of morphine and a brain-penetrant Angiopep-2-conjugated NT(8-13) improved the analgesic/adverse effect ratio.¹⁵

Since peptidic opioid ligands such as endomorphin-2 or dermorphin derivatives exert their opioid activity through their *N*-terminal residues and NT(1-13) *via* its six amino acids at the *C*-terminus, those two pharmacophores could potentially be fused in a straightforward fashion. To date, only one chimeric OP-NT peptide between a modified endomorphin-2 pharmacophore and an NT(8-13) analogue was described, namely, PK20 (Figure 2B).¹⁶ To yield PK20 starting from the native NT(8-13) sequence, Lys⁸ and Lys⁹ replaced the native Arg residues, Tyr¹¹ was substituted by a Phe, and Ile was changed for a Tle in order to improve enzymatic stability. Additionally, the *N*-terminal endomorphin-2 pharmacophore was modified to improve both enzymatic stability and affinity to the opioid receptors *via* incorporation of a 2',6'-dimethyltyrosine residue (Dmt) and substitution of Pro for *D*-Lys.¹⁶ This decapeptide was tested *in vivo* in the rat tail-flick test and showed a long-lasting, time-dependent antinociceptive activity. Antinociception resulted from an additive effect of the two antinociceptive systems, opioid and NT, since naltrexone administration only partially reduced the antinociceptive activity of PK20.¹⁶ More recently, it was reported that the analogue [Ile⁹]PK20 (Figure 2B), which shows a lowered potency *in vivo* when compared to the combination of both pharmacophores, causes less side effects, such as motor incoordination.¹⁷

Herein, we describe the design, synthesis, pharmacological evaluation, and structure–activity relationship (SAR) studies of a series of new OP-NT analogues (Figure 3). The OP-NT

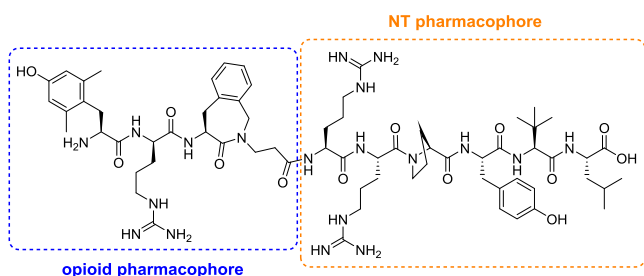


Figure 3. Design strategy of new OP-NT hybrid peptides (with the 4-amino-1,2,4,5-tetrahydro-3H-benzo[*c*]azepin-3-one “Aba” residue in the third position of the sequence).

hybrid peptides were designed by fusing an MOR agonist derived from dermorphin and featuring an aminobenzazepinone (Aba) as a constrained Phe mimetic, KGOP01 (H-Dmt-*D*-Arg-Aba- β -Ala-NH₂), and NT(8-13) derivatives (Figure 3). This specific opioid segment was previously described as a balanced MOR/DOR agonist with better affinities and activities than the reference peptide [Dmt¹]DALDA.¹⁸ The important role of the Dmt¹ residue in KGOP01 on ligand binding and activation of the MOR was also highlighted in a very recent molecular modeling study.^{18c} In addition to a high metabolic stability and BBB permeation, the opioid tetrapeptide KGOP01 has been efficiently fused to other pharmacophores, including neuropeptide FF, neurokinin, and nociceptin antagonists, leading to bifunctional ligands with interesting pharmacological profiles.^{18b,19} In the present study, in the search for potent MOR-NTS ligands, several NT sequence modifications, particularly on Tyr¹¹ and the two basic residues Arg⁸ and Arg⁹, were targeted in order to retain binding at the MOR and NT receptors. To this aim, pharmacological investigations were undertaken to evaluate the consequences of merging NT(8-13) analogues with the opioid agonist KGOP01 pharmacophore on binding to the opioid and NT receptors as well as activities at the opioid and NTS1 receptor, and the emerged SARs are reported.

RESULTS AND DISCUSSION

Design and Synthesis. In this study, we have designed OP-NT chimeric ligands based on a combination of the MOR/DOR agonist KGOP01 and NT(8-13) analogues (Figure 3 and Table 1). In order to preserve binding to both receptor types, the two pharmacophores were fused *via* a peptide bond between the *C*-terminal β -Ala residue of KGOP01 and the first basic *N*-terminal residue of the NT(8-13) analogues.

Based on previous studies, published by our group and others, several modifications were introduced within the NT(8-13) native sequence.²⁰ For example, the benefit of a Tle residue in lieu of the native Ile¹² to improve proteolytic stability had been previously demonstrated.²¹ Moreover, several studies highlighted the crucial importance of the aromatic residue in position 11 for NTS2 selectivity.²² Since our recent results indicated that Dmt, (6-OH)Tic, and *m*-Tyr substitutions were well tolerated and led to an increased NTS2 selectivity,¹¹ those modifications were also introduced in the OP-NT chimeric analogues. For the same reason, modification was attempted within the dibasic *N*-terminal motif of NT(8-13) through insertion of a β^3 -homo amino acid in position 8.²³ Knowing that the substitution of Arg⁸-Arg⁹ for Lys residues has

Table 1. OP-NT Hybrid Peptides Designed and Investigated in the Present Study^a

compound number	sequence
3	H-Dmt- <i>D</i> -Arg-Aba- β -Ala-Arg-Arg-Pro-Tyr-Tle-Leu-OH
4	H-Dmt- <i>D</i> -Arg-Aba- β -Ala-Lys-Lys-Pro-Tyr-Tle-Leu-OH
5	H-Dmt- <i>D</i> -Arg-Aba- β -Ala-Arg-Arg-Pro-Dmt-Tle-Leu-OH
6	H-Dmt- <i>D</i> -Arg-Aba- β -Ala-Lys-Lys-Pro-Dmt-Tle-Leu-OH
7	H-Dmt- <i>D</i> -Arg-Aba- β -Ala- β^3 hArg-Arg-Pro-Dmt-Tle-Leu-OH
8	H-Dmt- <i>D</i> -Arg-Aba- β -Ala- β^3 hLys-Lys-Pro-Dmt-Tle-Leu-OH
9	H-Dmt- <i>D</i> -Arg-Aba- β -Ala-Arg-Arg-Pro-(6-OH)Tic-Tle-Leu-OH
10	H-Dmt- <i>D</i> -Arg-Aba- β -Ala-Lys-Lys-Pro-(6-OH)Tic-Tle-Leu-OH
11	H-Dmt- <i>D</i> -Arg-Aba- β -Ala-Arg-Arg-Pro- <i>m</i> -Tyr-Tle-Leu-OH
12	H-Dmt- <i>D</i> -Arg-Aba- β -Ala-Lys-Lys-Pro- <i>m</i> -Tyr-Tle-Leu-OH

^aAll sequence modifications are highlighted in bold.

Table 2. Binding Affinities of OP-NT Hybrids and Reference Peptides to the Human Opioid and NT Receptors

peptide	affinity K_i (nM) ^a					selectivity NTS2/NTS1
	MOR	DOR	KOR	NTS1	NTS2	
KGOP01 ^b	0.14 ± 0.06	1.51 ± 0.26	16.6 ± 5.7	N/A ^d	N/A ^d	N/A ^d
NT(8-13) ^c	N/A ^d	N/A ^d	N/A ^d	0.90 ± 0.03	0.55 ± 0.2	1.6
PK20	4.13 ± 1.4	46.4 ± 3.6	33.5 ± 6.2	188 ± 29	29.5 ± 11	6.4
1 ^c	N/A ^d	N/A ^d	N/A ^d	3.6 ± 0.4	0.46 ± 0.03	7.8
2 ^c	N/A ^d	N/A ^d	N/A ^d	3790 ± 1300	2.86 ± 1.3	1324
3	1.32 ± 0.45	56.4 ± 4.5	78.6 ± 20	0.43 ± 0.07	0.09 ± 0.07	4.8
4	4.89 ± 0.30	213 ± 44	201 ± 80	2.3 ± 0.4	0.29 ± 0.2	7.7
5	1.11 ± 0.39	159 ± 94	102 ± 8.0	0.78 ± 0.2	0.03 ± 0.03	27
6	7.15 ± 0.83	276 ± 42	138 ± 16	13 ± 1.3	0.16 ± 0.05	81
7	1.75 ± 0.43	101 ± 2.0	27.9 ± 4.1	4.0 ± 0.05	0.003 ± 0.001	1333
8	7.12 ± 2.0	48.6 ± 5.7	208 ± 76	15 ± 2	0.32 ± 0.5	50
9	1.67 ± 0.16	105 ± 35	22.4 ± 1.6	4710 ± 580	1.72 ± 4.0	2739
10	6.24 ± 0.48	209 ± 25	150 ± 53	6830 ± 4000	75.0 ± 80	91
11	1.73 ± 0.62	60.9 ± 8.6	19.9 ± 4.2	12.4 ± 0.9	0.33 ± 0.04	33
12	3.99 ± 0.97	200 ± 73	70.9 ± 15	59 ± 1.5	0.50 ± 0.45	118
13 ^c	N/A ^d	N/A ^d	N/A ^d	2.3 ± 0.2	0.11 ± 0.07	20.1
14 ^c	N/A ^d	N/A ^d	N/A ^d	13.4 ± 2.0	3.0 ± 2.0	4.5
15 ^c	N/A ^d	N/A ^d	N/A ^d	6680 ± 3700	132 ± 47	50
16 ^c	N/A ^d	N/A ^d	N/A ^d	93.0 ± 22	24.0 ± 18	4

^aDetermined in competitive radioligand binding assays using membranes from CHO cells (opioid and NTS1 receptors) or 1321N1 astrocytoma cells (NTS2 receptors) stably expressing the human receptors. K_i values are reported as the means ± SEM of three independent experiments performed in duplicate (binding to the opioid receptors) or triplicate (binding to the NT receptors). ^bData taken from ref 25. ^cData taken from ref 11. ^dN/A, not applicable.

been shown to be beneficial for NTS2 selectivity and activity in nonconjugated NT analogues lacking a second pharmacophore,¹¹ this modification was also introduced in the design and synthesis of OP-NT hybrid peptides (Table 1).

Here, all chimeric structures were synthesized by solution phase peptide synthesis (SPPS) following the Fmoc/*t*-Bu methodology using HBTU/DIPEA or DIC/Oxyma Pure as coupling mixtures.²⁴ The first attempts were performed with a preloaded Fmoc-Leu-Wang resin (0.83 mmol/g loading), resulting in inefficient coupling from the Pro residue onward. This low reactivity became even more critical during the opioid tetrapeptide assembly on resin with coupling conversions remaining under 60%. This resulted in very complex mixtures of deletion peptides and cumbersome purification by RP-HPLC, therefore tremendously reducing the synthetic yield.

In order to facilitate the purification, a fragment strategy was attempted. The opioid tetrapeptide was thus assembled on a 2-chlorotrityl resin and cleaved with an HFIP/DCM mixture. The resulting fully protected peptide was obtained in good yield without need for further purification and coupled on the resin-bound NT sequence. Although it resulted in a facilitated purification, the conversion was limited to 40% and the fragment approach was not retained as a decent alternative. In an attempt to improve the peptide assembly, the polystyrene-based Wang resin was replaced with a 0.25 mmol/g Fmoc-Leu-Wang TentaGel resin. Gratefully, due to the reduced loading and PEG enting, this resin gave easier coupling steps (2 to 4 h with 1.5 equiv of amino acid for challenging peptide bond formations) with both HBTU/DIPEA and DIC/Oxyma Pure as coupling cocktails. All the analogues prepared in this work were cleaved from the resin with a TFA/TIS/H₂O 95:2.5:2.5 cleavage cocktail. After preparative HPLC purification, all NT analogues were obtained in yields ranging from 2.5 to 31% with an excellent purity (>95%).

In Vitro Binding Affinities and Selectivities. Binding affinities at the human opioid receptors (μ -(MOR), δ -(DOR), and κ -(KOR)) and NT receptors (NTS1 and NTS2) of the new OP-NT hybrid peptides (Table 1) were first determined in competitive radioligand binding assays using membranes from Chinese hamster ovary (CHO) or 1321N1 astrocytoma cells stably expressing one of the recombinant human receptors (CHO cells for opioid and NTS1 receptors and 1321N1 cells for NTS2 receptors), according to the described procedures.^{11,25} For comparison purposes, binding profiles of the reference peptides KGOP01, NT(8-13), 1, 2, and PK20 to opioid and NT receptors are presented (Table 2 and Figures S1 and S2).

In vitro binding studies demonstrated that the addition of an NT sequence to the opioid tetrapeptide C-terminus affects binding to the opioid receptors (Table 2). We observed that the extra hexapeptide reduces MOR, DOR, and KOR binding, as compared to the parent opioid agonist KGOP01 (at least 8- and 32-fold decreases for the MOR and DOR, respectively, and up to a 12-fold decrease for the KOR). Overall, the observed drop in binding affinities shown by the OP-NT hybrids versus KGOP01 was less at the MOR compared to affinities at the DOR and KOR, with the hybrid peptides still exhibiting K_i values at the MOR in a satisfactory low nanomolar range (1.11–7.15 nM) and showing MOR selectivity (Table 2). Several of the new OP-NT hybrid peptides showed increased or comparable MOR binding affinities to PK20 ($K_i = 4.13$ nM). Additionally, modifications of the Tyr residue from the native NT sequence have no effect on the MOR binding and minor influence on DOR and KOR affinities, without an apparent pattern. Nonetheless, the two basic residues of the NT pharmacophore seem to be impactful on opioid receptor binding since their substitution by Lys residues generally resulted in reduced binding affinity. For example, peptide 10 shows around 4-, 2-, and 7-fold decreases

Table 3. *In Vitro* Functional Activities of OP-NT Hybrid Peptides and Reference Peptides to the Human Opioid and NT Receptors

compound code/number	<i>in vitro</i> agonist activity ^a									
	MOR [³⁵ S]GTPγS binding		MOR β-arrestin-2 recruitment		DOR [³⁵ S]GTPγS binding		KOR [³⁵ S]GTPγS binding		NTS1 Gαq activation	
	EC ₅₀ (nM)	E _{max} (%)	EC ₅₀ (nM)	E _{max} (%)	EC ₅₀ (nM)	E _{max} (%)	EC ₅₀ (nM)	E _{max} (%)	EC ₅₀ (nM)	E _{max} (%)
KGOP01	0.10 ± 0.03	100 ± 7	5.53 ± 0.61	107 ± 2	1.27 ± 0.76	104 ± 14	>10,000	N.D. ^c	N/A ^b	N/A ^b
NT(8-13)	N/A ^b	N/A ^b	N/A ^b	N/A ^b	N/A ^b	N/A ^b	N/A ^b	N/A ^b	0.15 ± 0.03	100 ± 6
PK20	13.3 ± 3.2	91 ± 3	956 ± 100	69 ± 4	479 ± 127	78 ± 2	47.1 ± 10	65 ± 8	19.1 ± 3.9	101 ± 3
1	N/A ^b	N/A ^b	N/A ^b	N/A ^b	N/A ^b	N/A ^b	N/A ^b	N/A ^b	1.70 ± 0.6	97 ± 10
3	12.8 ± 5.0	94 ± 6	1329 ± 365	72 ± 4	301 ± 41	106 ± 3	514 ± 7.0	34 ± 3	0.24 ± 0.2	111 ± 7
4	64.6 ± 15	99 ± 6	2459 ± 219	67 ± 6	1320 ± 67	87 ± 4	1649 ± 144	31 ± 3	0.26 ± 0.1	99 ± 17
5	9.12 ± 1.1	96 ± 2	1142 ± 187	79 ± 6	313 ± 61	91 ± 6	415 ± 56	37 ± 3	1.3 ± 0.5	101 ± 12
6	48.7 ± 14	95 ± 4	1965 ± 528	62 ± 1	898 ± 187	60 ± 5	1574 ± 681	22 ± 2	3.9 ± 1	109 ± 15
7	28.7 ± 8.8	94 ± 2	1066 ± 306	68 ± 3	305 ± 71	99 ± 4	158 ± 82	46 ± 6	0.86 ± 0.6	114 ± 16
8	65.4 ± 6.5	97 ± 2	3044 ± 526	69 ± 6	248 ± 81	97 ± 5	239 ± 62	36 ± 5	1.8 ± 1	112 ± 10
9	4.56 ± 0.25	98 ± 5	934 ± 82	67 ± 5	227 ± 8.0	97 ± 3	399 ± 69	20 ± 6	1900 ± 100	74 ± 11
10	45.6 ± 13	94 ± 3	2163 ± 99	66 ± 2	842 ± 86	91 ± 0.3	1556 ± 852	20 ± 3	N.D. ^c	N.D. ^c
11	6.49 ± 1.3	95 ± 6	359 ± 70	81 ± 3	177 ± 36	110 ± 2	424 ± 146	28 ± 4	6.7 ± 4	95 ± 6
12	27.4 ± 9.4	87 ± 2	1271 ± 153	66 ± 5	452 ± 118	90 ± 2	401 ± 50	30 ± 5	15 ± 7	90 ± 13

^aDetermined in the [³⁵S]GTPγS binding assays using membranes from CHO cells stably expressing the human opioid receptors, in the PathHunter β-arrestin-2 recruitment assay with U2OS cells coexpressing the hMOR and the enzyme acceptor-tagged β-arrestin-2 fusion protein, or in the bioluminescence resonance energy transfer (BRET)-based assay conducted in HEK293 cells transiently transfected with hNTS1 and BRET biosensors. E_{max} values are expressed as the percentage relative to the reference agonists DAMGO (MOR), DPDPE (DOR), U69,593 (KOR), and NT(8-13) (NTS1). Data are means ± SEM of three independent experiments performed in duplicate (activity to the opioid receptors) or triplicate (activity to the NTS1 receptor). ^bN/A, not applicable. ^cN.D., no detectable signal.

in binding affinity to the MOR, DOR, and KOR, respectively, as compared to the Arg-containing sequence **9** (Table 2). Thus, fusion of the opioid and NT pharmacophores modifies the pharmacological profile at the opioid receptors converting a balanced MOR/DOR ligand (KGOP01) into more MOR-selective ligands, as shown by the new OP-NT hybrid peptides (Table 2).

Additionally to PK20, described as an opioid-NT hybrid peptide,^{16,17,26} the binding profile at the NT receptors of the newly designed OP-NT hybrids (Table 1) was evaluated. Conversely to the interaction with the opioid receptors, the addition of the opioid tetrapeptide at the N-terminus of NT sequences seems to be well tolerated for binding at NT receptors (Table 2). We observed that peptide **3** shows a higher binding at both NTS1 and NTS2 than the parent NT pharmacophore (K_i values of 0.43 and 0.09 nM, respectively) but has a minor effect on NTS2 selectivity (4.8 vs 7.8 for **1**) (Table 2). This observation is consistent with the crystal structure of NTS1 bound to NT(8-13) described by White *et al.*²⁷ While the residues Ile¹² and Leu¹³ are deeply buried in a hydrophobic pocket, the N-terminal Arg⁸ is localized at receptor's surface and appears to be relatively free in terms of positioning. Therefore, peptide backbone elongation *via* conjugation with the opioid tetrapeptide is not impairing NTS1 nor NTS2 binding.

As expected, ligands with favorable selectivity toward NTS2 were obtained by introducing Tyr¹¹ modifications, a residue which is of crucial importance for NT receptor selectivity. Accordingly, hybrids bearing a Dmt (**5**), (6-OH)Tic (**9**), or *m*-Tyr (**11**) residue show a reduced binding at NTS1 while retaining a good affinity at NTS2, therefore reaching higher selectivity (up to 2739 for peptide **9**) than the NT pharmacophore alone.¹¹ This observation is consistent with our recent findings indicating that those modifications in

NT(8-13) analogues induced superior NTS2 selectivity, particularly when incorporating (6-OH)Tic, as shown by **9**, which exhibits a large decrease in affinity at NTS1 (K_i = 4.7 μM). The addition of an extra methylene group within the peptide backbone *via* the use of a β³-homo amino acid also led to major changes in NT receptor binding. This effect was particularly noticeable for **7**, bearing a β³hArg residue and showing a 5-fold decrease in affinity at NTS1 and a 10-fold increase in NTS2 binding, as compared to the α-amino acid bearing sequence (**5**). Intriguingly, the opioid pharmacophore seems to play a role in this superior affinity and selectivity for NTS2 when compared to the parent NT ligand alone, peptide **13** (H-β³hArg-Arg-Pro-Dmt-Tle-Leu-OH; Table 2). Indeed, the addition of the tetrapeptide at the C-terminus led to a 2-fold decrease in affinity for NTS1 and 37-fold improved binding at NTS2. Peptide **7** reached the best NTS2 affinity reported so far with a K_i in the picomolar range (K_i = 3 pM) and having a substantially increased NTS2 selectivity (from 27 to 1333) (Table 2). Moreover, comparison of these analogues with their NT parents (**7** vs **13**; **5** vs **14**, H-Arg-Arg-Pro-Dmt-Tle-Leu-OH; **9** vs **15**, H-Arg-Arg-Pro-(6-OH)Tic-Tle-Leu-OH; and **11** vs **16**, H-Arg-Arg-Pro-*m*-Tyr-Tle-Leu-OH) shows that the addition of the opioid tetrapeptide is beneficial for most of the hybrid analogues, both in terms of NTS2 binding and selectivity. Interestingly, Arg substitutions by Lys residues did not induce the expected improvement, as observed with NT analogues alone.¹¹ Actually, these hybrids generally showed a slightly reduced binding at NTS1 but different effects were noticed at NTS2, namely, decreased (for **8** vs **7** and **10** vs **9**) or similar affinity (for **12** vs **11**). Therefore, this modification has no consistent influence on NTS2 selectivity in case of chimeric structures.

The above results are also in line with the poor binding profile for PK20 at NT receptors (Table 2). Indeed, this

previously described OP-NT hybrid shows much reduced affinities compared to most of the new analogues (with K_i values of 188 and 29.5 nM at NTS1 and NTS2, respectively) and a modest selectivity for NTS2 (6.4-fold). Contrary to the binding profile at the MOR for which the newly prepared OP-NT hybrids show a roughly 2-fold improvement as compared to PK20, their affinities for the NT receptors and selectivities for NTS2 have been significantly improved, particularly due to the introduction of a (6-OH)Tic residue (peptide 9) or Dmt and β^3 hArg residues (peptide 7, Table 2).

In Vitro Functional Activities. The *in vitro* functional opioid profile of the new OP-NT hybrid peptides (3–12) to the human opioid receptors was next determined in the guanosine-5'-O-(3-[35 S]thio)-triphosphate ([35 S]GTP γ S) binding assays using membranes from CHO cells stably expressing the human MOR, DOR, or KOR, performed as described.²⁸ Generally, lower MOR potencies were observed for the new OP-NT hybrids when compared to the parent opioid tetrapeptide KGOP01, with the largest decreases observed in DOR and KOR agonist potencies (Table 3). Furthermore, the *in vitro* functional results correlate well with the observations from radioligand binding studies, with the addition of an NT sequence to the opioid tetrapeptide KGOP01 affecting both binding and activation of the opioid receptors.

Based on functional activities at the MOR, several OP-NT ligands were very potent agonists (3, 5, 9, and 11) with all peptides acting as full agonists in inducing MOR-mediated G protein activation. As shown in Table 3, all hybrids showed full efficacies at the DOR (exception being 6) and lower potencies than at the MOR, while a partial agonist profile with very low potencies was noted at the KOR. In the [35 S]GTP γ S binding assays, PK20 was found as a potent full agonist at the MOR, a weak partial agonist at the DOR, and a relatively potent KOR partial agonist (Table 3). Several of the new OP-NT hybrids showed increased or similar agonist potencies at the MOR than PK20.

In line with the competition binding studies (Table 2), the different modifications introduced in the NT(8-13) sequence did not clearly influence the opioid activity except for the two basic residues. Replacement of the two native Arg residues always resulted in increased EC_{50} values at all three opioid receptors as compared to the Arg-containing sequences. For example, 10 showed a 10-, 2.3-, and 3.7-fold higher EC_{50} values at MOR, DOR, and KOR respectively, when compared to 9.

Over the past years, increased research efforts were directed to the development of biased agonists at the opioid receptors, which lead to preferential activation of G protein over G protein-independent pathways, principle among them being the β -arrestin-2 signaling.^{5c,29,30} Biased agonism at the MOR received particular attention as the MOR is the main opioid receptor type for achieving effective analgesia that results from the G protein-mediated signaling, while lower or no efficacy for recruiting β -arrestin-2 should reduce the undesirable side effects of opioid analgesics.^{5a,c,30}

In this study, we have evaluated the capability of OP-NT hybrid peptides 3–12 to promote MOR-mediated β -arrestin-2 signaling in the PathHunter β -arrestin-2 recruitment assay using U2OS cells coexpressing the human MOR and the enzyme acceptor-tagged β -arrestin-2 fusion protein.²⁵ As shown in Table 3, it was evident that all new OP-NT ligands, as well as PK20, exhibited much lower potencies and efficacies (acting as partial agonists) in inducing β -arrestin-2 trans-

location (EC_{50} values ranging between 359 and 3044 nM) than in the MOR-mediated G protein activation. When comparing efficacies (E_{max} values) in inducing β -arrestin-2 recruitment after MOR activation, the functional profile of OP-NT hybrids is distinct to that of the parent opioid ligand KGOP01, which effectively recruited β -arrestin-2 (EC_{50} = 5.53 nM; E_{max} = 107%) (Table 3). Furthermore, KGOP01 was reported as an unbiased full MOR agonist *in vitro* and *in vivo*,¹³ consistent with its liability profile to elicit the typical unwanted MOR-mediated side effects, including respiratory depression, constipation, hyperalgesia, analgesic tolerance, and withdrawal in rodents.^{13,19b}

The *in vitro* functional NT profile of the new OP-NT hybrid peptides was also assessed. To this end, the NTS1 canonical signaling pathway was monitored by a BRET-based G α q activation assay using human embryonic kidney 293 (HEK293) cells stably expressing the human NTS1.³¹ Even though the corresponding modifications within the NT sequence did reduce NTS1 binding for most analogues, their agonistic activity at the receptor remained similar to the initial NT pharmacophore NT(8-13) or the reference peptide 1, i.e., within a nanomolar range. Conversely, 9 showed a moderate activity at NTS1 with EC_{50} around 2 μ M, corresponding to a ca. 1000-fold decrease when compared to 1 and a 13,000-fold to NT(8-13). Likewise, 10 was not able to induce Gq activation. Therefore, incorporating (6-OH)Tic in lieu of the native Tyr seems to be beneficial for a reduced NTS1 activity at Gq. Even though the hydroxyl group position on the aromatic ring seems to slightly influence binding to NTS1, as determined by comparing 3 and 11, this modification combined with a tetrahydroisoquinoline conformational constraint as in 9 fundamentally changed the pharmacological profile at this receptor. The main limitation of the present study is the lack of characterization of the activities of OP-NT hybrids at NTS2. As opposed to NTS1, the signaling pathways associated to NTS2 activation are still controversial, showing species-dependent and cell type-specific pharmacology. For instance, depending on the mammalian cell-based expression systems used to decipher the signal transduction pathways associated to the receptor–ligand interaction, NT compounds including the NTS2-selective ligand levocabastine were found to behave as full, partial, or inverse agonists or even as competitive antagonists at NTS2 receptors.⁷ Likewise, we and others have found in the FLIPR assay that the two well-known nonpeptide pyrazole-based antagonists SR48692 and SR142948a, which are known to bind NTS2, exert full agonist activity.³² However, these two small-molecule ligands are well described to both antagonize the antinociceptive effects of NT-based analogues in various types of pains, including acute, tonic, and chronic pain.³³ Despite efforts of different research groups and companies, there is unfortunately no reliable available cell-based signaling assay to profile NTS2 agonist activity.

Antinociceptive Activity. First *in vivo* studies on the antinociceptive effects of the novel OP-NT hybrids in mice were performed. One of the most promising fusion hybrids, 7, as an MOR agonist, showing the highest NTS2 affinity described so far (K_i = 3 pM) combined with a very large NTS2 versus NTS1 selectivity (>1300) (Tables 1 and 2), was investigated in a model of thermal nociception, the tail-flick test in mice, after systemic subcutaneous (sc) administration. Furthermore, we have compared the antinociceptive effect of the new hybrid peptide 7 to the effect of the previously

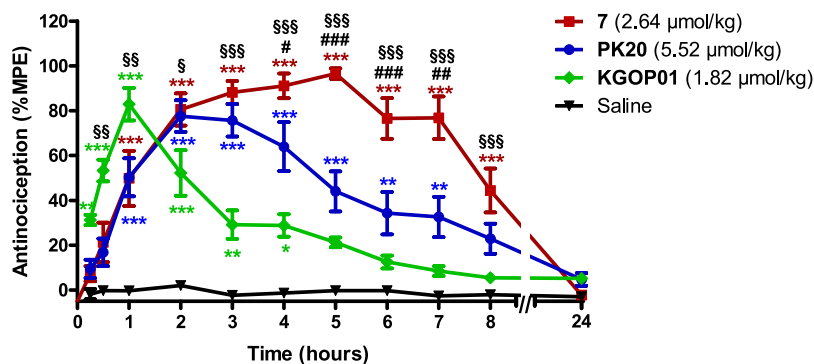


Figure 4. Comparison of antinociceptive effects of KGOP01 and OP-NT hybrids 7 and PK20 in the tail-flick test in mice after sc administration. Groups of mice were treated with KGOP01 (1.82 $\mu\text{mol/kg}$), 7 (2.64 $\mu\text{mol/kg}$), PK20 (5.52 $\mu\text{mol/kg}$), or saline (control), and tail-withdrawal latencies were measured at different time points after drug administration. Data are shown as means \pm SEM ($n = 5$ to 6 mice per group). $**P < 0.01$ and $***P < 0.001$ vs saline group; $\#P < 0.05$, $\#\#P < 0.01$, and $\#\#\#P < 0.001$ hybrid 7 vs PK20; $\$P < 0.01$ and $\$\$\$P < 0.001$ hybrid 7 vs KGOP01; two-way ANOVA with the Bonferroni post hoc test.

reported OP-NT hybrid PK20 and the opioid agonist KGOP01, which can be considered as the “parent” opioid segment in the reported hybrids. As shown in Figure 4, 7 (2.64 $\mu\text{mol/kg}$) increased tail-withdrawal latencies to thermal stimulation, with a significant and long-lasting antinociceptive effect up to 8 h after sc administration to mice. Notably, 7 showed an antinociceptive efficacy with $\geq 80\%$ of the maximum possible effect (%MPE) between 2 and 7 h. In line with earlier reports,^{16,26} PK20 (5.52 $\mu\text{mol/kg}$) produced also significant antinociception in the tail-flick test after systemic administration, reaching an 80% MPE at 2 and 3 h, which declined rapidly thereafter. Characteristic differences were observed in the time course of the antinociceptive effect of OP-NT hybrids 7 and PK20, sc given to mice in equianalgesic doses. Although both peptides had a similar time course up to 3 h reaching an 80% MPE at 2–3 h, 7 exhibited a significant and extended duration of action than PK20 (Figure 4). In this study, we also show that the addition of an NT sequence to the opioid tetrapeptide KGOP01, reported to produce antinociception of relatively short duration (peak effect at 1 h, with 80% MPE and fast decline) in the tail-flick test in mice after sc administration,¹³ resulted in the OP-NT hybrid, 7, that produced a considerably prolonged antinociceptive effect (up to 8 h) (Figure 4). It may be assumed that the antinociceptive effect of compound 7 up to 1 h is primarily due to MOR activation, between 2–4 h due to synergistic MOR-NT receptor activation and from 5 to 8 h due to NT receptor activation. The long duration of action of peptide analogue 7 correlates well with its half-life time ($t_{1/2} = 467 \pm 23$ min), determined in *in vitro* biostability experiments performed in human plasma at 37 °C. Despite its high affinity and selectivity for NTS2, we cannot, however, exclude that part of the antinociceptive activity of hybrid peptide 7 may be mediated through NTS1 binding since hybrid 7 still exhibits high affinity at the NTS1 ($K_i = 4$ nM).

CONCLUSIONS

In this study, we have reported the design, synthesis, *in vitro/in vivo* pharmacology, and SAR of new OP-NT multitarget peptides, which, unlike the single OP-NT chimeric structure known to date, PK20 derived from endomorphin-2, are associating a dermorphin derivative, KGOP01 as the opioid pharmacophore, and several NT analogues. On the basis of the emerged SAR studies, we have identified high-affinity MOR-

NT hybrid peptides, showing prolonged antinociceptive effects after systemic sc administration in mice. We have shown that fusion of the OP and NT pharmacophores appeared to largely alter the interaction with the opioid receptors with overall decreased binding at the DOR and KOR while maintaining a good affinity at the MOR. On the contrary, the addition of the opioid tetrapeptide at the *N*-terminus of NT(8–13) was highly beneficial for NT receptor binding in all cases, probably due to the fact that this opioid part is not interfering with the ability of the OP-NT hybrids to interact with either NTS1 or NTS2. As for pure NT analogues, incorporation of (6-OH)Tic or Dmt residues in lieu of the native Tyr¹¹, as well as a β^3 -homo amino acid in position 8, led to increased binding at NTS2. Particularly, combination of β^3 hArg and Dmt residues resulted in the OP-NT hybrid peptide 7, as a selective and full MOR agonist, showing the highest NTS2 affinity described to date ($K_i = 3$ pM) and a very good NTS2 versus NTS1 selectivity (>1300). The (6-OH)Tic-containing analogue 9 also exhibited high affinity, full agonism, and selectivity at the MOR, combined with good NTS2 affinity ($K_i = 1.7$ nM), and very low binding NTS1 affinity ($K_i = 4.7$ μM) and weak agonist activity at the NTS1, thus resulting in an excellent NTS2 selectivity (>2700). While all OP-NT multitarget ligands were potent full MOR agonists in activating the G protein signaling pathway, they behaved as partial agonists with much lower potencies in inducing β -arrestin-2 recruitment upon MOR activation. In addition, *in vivo* studies demonstrated that the hybrid 7 produced significant and prolonged antinociceptive effects (up to 8 h) in the tail-flick test after sc administration in mice, a profile supported by its high plasma stability. Comparison with KGOP01 and PK20 revealed that the new OP-NT multitarget peptide 7 had a considerably longer duration of the therapeutic antinociceptive effect, hence demonstrating the advantage of the new OP-NT hybrid design presented in this study for pain treatment. In summary, such multitarget ligands with a balanced combination of MOR agonism and high NTS receptor binding may represent new and safer analgesic drugs with improved pharmacology, and further *in vivo* studies evaluating the adverse effect profile will be published elsewhere.

EXPERIMENTAL SECTION

Chemistry. General Methods. For SPPS, usual *N*-Fmoc-protected amino acids (Leu, Tyr, Pro, Lys, and Arg) and *m*-Tyr were purchased from Chem-Impex (Wood Dale, USA). Tle was purchased from

Novabiochem (Merck Millipore, Burlington, USA), Boc-Dmt-OH from AstaTech (Bristol, USA), β^3 hLys from Anand Chem (Piestany, Slovakia), and β^3 hArg from abcr (Karlsruhe, Germany). DIC, HBTU, HOBt, Oxyma Pure, TFA, and TIS were purchased from Fluorochem (Hadfield, UK) and 4-methylpiperidine and DIPEA from Aldrich (St. Louis, USA). Resins used were Fmoc-Leu-Wang resin (0.827 mmol/g, method A) purchased from Chem-Impex (Wood Dale, USA) and Fmoc-Leu-Wang TG resin (0.25 mmol/g, method B) from Iris Biotech (Marktredwitz, Germany). ^1H and ^{13}C NMR spectra were recorded at 500 and 125 MHz on a Bruker Avance II 500 (Bruker Corp., Billerica, MA) or at 250 and 63 MHz on a Bruker Avance DRX 250 system. In the recorded spectra, tetramethylsilane (TMS) was used as the internal standard. The chemical shifts (δ) are expressed as parts per million (ppm), whereas the coupling constants (J) are given in hertz (Hz). HRMS analyses were recorded with a Micromass Q-ToF micro system using reserpine as a reference. HPLC preparative purifications were done with a ReproSil Pur 120 ODS-3 150 \times 16 mm (10–50% gradient in 10 min with ACN and H_2O + 0.1% TFA as eluent) column. Analytical HPLCs were done with a Chromolith HR C18 50 \times 4.6 column and LC-MS with an Acclaim 300 C18 2.1 \times 150 column.

Building Block Synthesis. Syntheses of Fmoc-protected building blocks Fmoc-Aba- β -Ala-OH,^{19a} Fmoc-*m*-Tyr-OH,¹¹ and Fmoc-(6-OH)Tic-OH³⁴ were performed as described previously.

Phth-Phe- β -Ala-OEt. Phthaloyl-protected phenylalanine **16** (5 g, 16.9 mmol) was dissolved in 80 mL of CH_2Cl_2 . β -Alanine ethyl ester hydrochloride (β -Ala-OEt-HCl; 2.86 g, 18.6 mmol) and coupling reagent TBTU (5.98 g, 18.6 mmol) were added. Et_3N (7.08 mL, 50.8 mmol) was added to the solution, and the pH was kept at pH 8 by the use of Et_3N . The solution was then stirred for 1 h. The solvent was evaporated, and the residue was dissolved in ethyl acetate. The solution was then washed with 1 N HCl solution (3 \times), saturated NaHCO_3 solution (3 \times), and brine (3 \times). The organic phase was dried with MgSO_4 , filtered, and evaporated *in vacuo*. The resulting residue was crystallized from a minimum amount of warm ethanol. After cooling down and filtration, white crystals were obtained after two subsequent crystallizations (4.64 g, 70%).

^1H NMR (CDCl_3 , 500 MHz): δ (ppm) 1.23 (t, J = 7.1 Hz, 3H), 2.53 (m, 2H), 3.54 (m, 4H), 4.09 (q, J = 7.1 Hz, 2H), 5.08 (dd, J = 10.4, 6.3 Hz, 1H), 6.70 (m, 1H), 7.04–7.23 (m, 5H), 7.63–7.82 (m, 4H). ^{13}C NMR (CDCl_3 , 125 MHz): δ (ppm) 14.1, 33.7, 34.7, 35.2, 55.7, 60.8, 123.5, 126.9, 128.6, 128.9, 131.4, 134.2, 136.7, 167.8, 168.4, 172.5.

Phth-Aba- β -Ala-OEt. To a 1 L dried two-neck round-bottom flask equipped with dried Dean–Stark apparatus and a dried cooler, P_2O_5 (40 g, 281.9 mmol), benzene (300 mL), acetic acid (200 mL), and 85% H_3PO_4 (9.1 mL, 135.9 mmol) were added. The mixture is then reflux (115 $^\circ\text{C}$) for 1 h. After letting the mixture to cool down, dried Phth-Phe- β -Ala-OH (5g, 12.7 mmol) and 1,3,5-trioxane (7.6 g, 83.8 mmol) were added and the mixture was again refluxed at 115 $^\circ\text{C}$. Every 30 min to 1 h, 1,3,5-trioxane (7.6 g, 83.8 mmol) was added. The reaction was monitored every 30 min to 1 h by HPLC. After complete consumption of the dipeptide, the reaction mixture was cooled down and benzene is evaporated *in vacuo*. The residue was dissolved in AcOEt and washed with 1 M HCl (3 \times), then with a saturated NaHCO_3 solution (6 to 8 \times , until pH 7), and twice with brine. The resulting organic phase was dried with MgSO_4 , filtered, and concentrated under reduced pressure. The crude was purified by manual column chromatography using petroleum ether/AcOEt 7:3 then 1:1, yielding the final compound (3.24 g, 63%) as a pale yellow solid.

^1H (CDCl_3 , 500 MHz): δ (ppm) 1.22 (t, J = 7.2 Hz, 3H), 2.62 (m, 2H), 3.12 (dd, J = 15.6, 4.7 Hz, 1H), 3.74 (m, 1H), 3.89 (m, 1H), 4.11 (m, 1H), 4.71 (d, J = 15.8 Hz, 1H), 4.78 (d, J = 15.9 Hz, 1H), 5.36 (dd, J = 13.1, 4.9 Hz, 1H), 7.25–7.30 (m, 4H), 7.75 (m, 2H), 7.89 (m, 2H). ^{13}C NMR (CDCl_3 , 125 MHz): δ (ppm) 14.1, 33.2, 34.1, 46.6, 52.0, 53.0, 60.7, 123.5, 127.1, 128.5, 128.7, 130.0, 132.0, 134.1, 135.6, 135.9, 168.0, 168.6, 172.0.

Phth-Aba- β -Ala-OH. Phth-Aba- β -Ala-OEt (4.74 g, 11.7 mmol) was dissolved in 60 mL of acetone. Then, 60 mL of a 1 N HCl solution

was slowly added. The mixture was refluxed in an oil bath at 90 $^\circ\text{C}$ for 16 h and then cooled to room temperature, and finally, the solvent was evaporated *in vacuo*. A white solid was obtained in quantitative yield and was used in the next step without purification.

^1H NMR (CDCl_3 , 500 MHz): δ (ppm) 2.68 (m, 2H), 3.10 (dd, J = 15.5, 4.8 Hz, 1H), 3.72 (m, 1H), 3.88 (m, 1H), 4.11 (dd, J = 15.5, 13.7 Hz, 1H), 4.73 (pseudo-s, 2H), 5.32 (dd, J = 13.0, 4.9 Hz, 1H), 7.22–7.32 (m, 4H), 7.73 (m, 2H), 7.87 (m, 2H). ^{13}C NMR (CDCl_3 , 125 MHz): δ (ppm) 32.9, 34.2, 46.6, 52.1, 53.2, 123.6, 127.3, 128.4, 128.8, 130.0, 132.0, 134.2, 135.6, 135.8, 167.9, 168.8, 175.7.

Fmoc-Aba- β -Ala-OH. To a 50 mL round-bottom flask, Phth-Aba- β -Ala-OH (0.958 g, 2.53 mmol) and hydrazine monohydrate (0.740 mL, 15.2 mmol) in EtOH (25 mL) were added to give a yellow solution. The reaction mixture was refluxed at 90 $^\circ\text{C}$ for 2 h. After solvent evaporation under reduced pressure, 10 mL of water was added to the residue. The pH was adapted to 5 by means of acetic acid additions. The mixture was then stirred for 30 min at rt, filtered, and concentrated under reduced pressure to yield the phthaloyl-protected intermediate as a yellow solid (1.16 g). The residue was then dissolved in water/acetone 1:1 (10 mL). Afterward, a solution of sodium carbonate (0.296 g, 2.79 mmol) and Fmoc-OSu (0.855 g, 2.53 mmol) in water/acetone (10 mL) was added to give a yellow suspension. The reaction mixture was stirred at rt for 18 h. The solvent was evaporated, and the resulting aqueous solution was acidified with 6 M HCl until pH 2. The aqueous phase was extracted with ethyl acetate (3 \times), and the resulting organic phase was washed once with brine, dried with MgSO_4 , filtered, and concentrated under reduced pressure. The residue was purified by column chromatography using 1% MeOH in DCM + 1% AcOH as eluent. The pure fractions were finally combined and evaporated, yielding, after trituration with diethyl ether (3 \times), the final compound as a white powder (0.870 g, 73% yield).

^1H NMR (CDCl_3 , 500 MHz): δ (ppm) 2.32 (m, 2H), 2.94 (dd, J = 17.1, 13.5 Hz, 1H), 3.18 (dd, J = 17.3, 4.5 Hz, 1H), 3.56 (m, 2H), 4.14 (d, J = 16.7 Hz, 1H), 4.24 (m, 1H), 4.31 (m, 2H), 5.08 (m, 1H), 5.13 (d, 1H). ^{13}C NMR (CDCl_3 , 125 MHz): δ (ppm) 33.3, 35.6, 43.9, 47.1, 50.2, 51.4, 66.3, 120.6, 125.8, 126.4, 127.6, 128.1, 128.1, 129.2, 131.0, 135.2, 135.9, 141.2, 144.4, 156.1, 171.5, 173.0.

Fmoc-*m*-Tyr-OH. To a round-bottom flask, *L-m*-Tyr (300 mg, 1.65 mmol) and $\text{H}_2\text{O}/\text{CH}_3\text{CN}$ (30 mL, 1:1) were added. Sodium carbonate (202 mg, 1.81 mmol) was added followed by Fmoc-OSu (574 mg, 1.65 mmol). The reaction mixture was stirred at room temperature under Ar for 4 h. Acetonitrile was then evaporated *in vacuo*, and the resulting aqueous solution was acidified to pH 2 by means of 1 M HCl addition and extracted by AcOEt (3 \times). The combined organic phases were then washed with brine, dried with MgSO_4 , filtered, and concentrated under reduced pressure. The crude was finally purified by column chromatography using petroleum ether/AcOEt 1:1 + 1% AcOH as eluent, yielding Fmoc-*m*-Tyr-OH (471 mg, 72%).

^1H NMR (250 MHz, CDCl_3): δ (ppm) 7.76 (d, J = 7.4 Hz, 2H), 7.55 (d, J = 7.4 Hz, 2H), 7.46–7.27 (m, 4H), 6.80–6.53 (m, 3H), 5.27 (d, J = 7.9 Hz, 1H), 4.73–4.58 (m, 1H), 4.53–4.31 (m, 2H), 4.25–4.15 (m, 1H), 3.22–2.98 (m, 2H). ^{13}C NMR (63 MHz, CDCl_3): δ (ppm) 173.89, 156.69, 156.17, 143.83, 143.75, 141.31, 137.47, 129.71, 127.78, 127.16, 125.18, 125.12, 121.22, 120.01, 116.05, 114.32, 67.13, 54.58, 47.12, 37.76.

Fmoc-(6-OH)Tic-OH. To a round-bottom flask, H-*m*-Tyr-OH (200 mg, 1.1 mmol), formalin 37% (150 μL , 1.85 mmol), and 0.05M H_2SO_4 (1.61 mL, 0.08 mmol) were added. The reaction mixture was heated (70 $^\circ\text{C}$) for 5 h, cooled down, and then filtered. The resulting brown solid was dried under vacuum, yielding the H-(6-OH)Tic-OH intermediate used without further purification.

H-(6-OH)Tic-OH was suspended in $\text{H}_2\text{O}/\text{CH}_3\text{CN}$ (20 mL, 1:1). Sodium carbonate (147 mg, 1.32 mmol) was then added (reaching pH 8) followed by Fmoc-OSu (386 mg, 1.1 mmol). The reaction mixture was stirred at room temperature under Ar for 1.5 h. Acetonitrile was evaporated *in vacuo*, and the resulting aqueous solution was acidified to pH 2 by means of 1 M HCl addition and extracted with AcOEt (3 \times). The combined organic phases were dried

with MgSO₄, filtered, and concentrated. The crude was finally purified by column chromatography using petroleum ether/AcOEt 1:1 + 1% AcOH as eluent, yielding the pure Fmoc-(6-OH)Tic-OH (127 mg, 28% in two steps).

¹H NMR (250 MHz, MeOD): δ (ppm) 7.87–7.72 (m, 2H), 7.71–7.54 (m, 2H), 7.49–7.22 (m, 4H), 6.93 (dd, J = 20.5, 8.1 Hz, 1H), 6.71–6.50 (m, 2H), 4.78 (dd, J = 5.8, 3.8 Hz, 1H), 4.60–4.39 (m, 4H), 4.38–4.18 (m, 1H), 3.15–3.04 ppm (m, 2H).

Peptide Synthesis. Peptides were synthesized manually by the standard Fmoc/*t*-Bu SPPS methodology in a plastic syringe. Fmoc removal was achieved using a 20% 4-methylpiperidine solution in DMF for 5 then 15 min. Standard amino acids were coupled using a 3-fold excess DIC (3 equiv) and Oxyma Pure or HOBT (3equiv) in DMF for 45 min at rt, while unnatural residues (Dmt, (6-OH)Tic, and *m*-Tyr) were coupled using 1.5 equiv for 1 h to one night. For Tlc coupling or 3 and 4 peptide assembly, this coupling mixture was replaced by HBTU (3 equiv) and DIPEA (5 equiv). Peptides **6** and **10** were synthesized on preloaded Fmoc-Leu-Wang resin (0.827 mmol/g, 121 mg), and Lys, Aba- β -Ala, D-Arg, and Dmt residues were coupled overnight at rt (method A). The other analogues were synthesized on a preloaded Fmoc-Leu-Wang TG resin (0.25 mmol/g, 400 mg), and Arg, Lys, β^3 hArg, β^3 hLys, Aba- β -Ala, DArg, and Dmt were coupled for 1–4 h (method B). All coupling steps were confirmed by Kaiser and Chloranil tests and/or small-scale cleavages followed by LC–MS analyses.

Peptide cleavages were performed with a TFA/TIS/H₂O 95:2.5:2.5 (v/v/v) solution at rt for 4 h. After TFA evaporation, crude peptides were precipitated in cold diethyl ether and then lyophilized overnight. The crude peptides were purified by preparative HPLC using a ReproSil Pur 120 ODS-3 150 \times 16 mm column (10–50% gradient in 10 min with ACN + 0.1% TFA and H₂O + 0.1% TFA as eluent). All peptide analogues were obtained in purity higher than 95%.

In Vitro Pharmacology. Materials and Chemicals. Cell culture media and supplements were obtained from Sigma-Aldrich Chemicals (St. Louis, MO) or Life Technologies (Carlsbad, CA). Radioligands [³H][D-Ala²,N-Me-Phe⁴,Gly-ol⁵]enkephalin ([³H]DAMGO, 50 Ci/mmol), [³H]diprenorphine (37 Ci/mmol), [³H]U69,593 (39.1 Ci/mmol), and [³⁵S]GTP γ S (1250 Ci/mmol) were purchased from PerkinElmer (Traiskirchen, Austria). [¹²⁵I]-NT (~2200 Ci/mmol) was purchased from PerkinElmer (Billerica, MA). DAMGO, [D-Pen²,D-Pen⁵]enkephalin (DPDPE), U69,593, diprenorphine, tris-(hydroxymethyl)aminomethane (Tris), 2-[4-(2-hydroxyethyl)-piperazin-1-yl]ethanesulfonic acid (HEPES), unlabeled GTP γ S, and guanosine diphosphate (GDP) were obtained from Sigma-Aldrich Chemicals (St. Louis, MO). PathHunter detection reagents were obtained from DiscoverX (Birmingham, UK). All other chemicals were of analytical grade and obtained from standard commercial sources. Test peptides were prepared as 1 mM stocks in water and further diluted to working concentrations in the appropriate medium.

Cell Cultures. CHO cells stably expressing the human opioid receptors, MOR, DOR, or KOR (CHO-hMOR, CHO-hDOR, and CHO-hKOR cell lines, respectively) were kindly provided by Dr. Lawrence Toll (SRI International, Menlo Park, CA). CHO-hMOR and CHO-hDOR cells were grown at 37 °C in the Dulbecco's modified Eagle's medium (DMEM)/Ham's F-12 culture medium supplemented with 10% fetal bovine serum, 0.1% penicillin/streptomycin, 2 mM L-glutamine, and 0.4 mg/mL G418. CHO-hKOR cells were grown at 37 °C in the DMEM culture medium supplemented with 10% fetal bovine serum, 0.1% penicillin/streptomycin, 2 mM L-glutamine, and 0.4 mg/mL G418. CHO-K1 cells stably expressing the human NTS1 receptor (ES-690-C from PerkinElmer, Montreal, Canada) and 1321N1 (human astrocytoma) cells stably expressing the human NTS2 receptor (ES-691-C from PerkinElmer, Montreal, Canada) were grown at 37 °C in the DMEM/F-12 culture medium supplemented with 10% fetal bovine serum, 10 IU penicillin, 100 μ g/mL streptomycin, 20 mM HEPES, and 0.4 mg/mL G418. HEK293 cells were maintained in the DMEM supplemented with 10% FBS, 100 IU/mL penicillin, and 100 μ g/mL streptomycin. U2OS cells stably coexpressing the human MOR and the enzyme acceptor (EA)-tagged β -arrestin-2 fusion protein

(USOS- β -arrestin-hMOR-PathHunter cells) (93-0213C3 from DiscoverX, Birmingham, UK) were cultured in the minimum essential medium (MEM) culture medium supplemented with 10% fetal bovine serum, 0.1% penicillin/streptomycin, 2 mM L-glutamine, 0.5 mg/mL G418, and 0.25 mg/mL hygromycin. All cell cultures were maintained in a humidified atmosphere of 95% air and 5% CO₂.

Competitive Radioligand Binding Assays for Opioid Receptors. Binding assays were conducted on human opioid receptors stably transfected into CHO cells according to the published procedures.²⁵ Briefly, CHO-hMOR, CHO-hDOR, and CHO-hKOR cells grown at confluence were removed from the culture plates by scraping, homogenized in 50 mM Tris-HCl buffer (pH 7.4), using a POLYTRON homogenizer, then centrifuged once, and washed by an additional centrifugation at 27,000g for 15 min at 4 °C. The final pellet was resuspended in 50 mM Tris-HCl buffer (pH 7.4), and cell membranes (15–20 μ g) were incubated with [³H]DAMGO (K_d = 1.59 nM), [³H]diprenorphine (K_d = 0.28 nM), or [³H]U69,593 (K_d = 1.62 nM) for labeling hMOR, hDOR and hKOR, respectively, and various concentrations of test peptides in a final volume of 1.0 mL for 60 min at 25 °C. Nonspecific binding was determined using 1–10 μ M of the unlabeled counterpart of each radioligand. Reactions were terminated by rapid filtration through Whatman glass GF/C fiber filters. Filters were washed three times with 5 mL of ice-cold 50 mM Tris-HCl buffer (pH 7.4) using a Brandel M24R cell harvester (Gaithersburg, MD). Radioactivity retained on the filters was counted by liquid scintillation counting using a Beckman Coulter LS6500 (Beckman Coulter Inc., Fullerton, CA). All experiments were performed in duplicate and repeated three times with independently prepared samples.

Competitive Radioligand Binding Assays for NTS1 and NTS2 receptors. Binding assays were conducted on human NTS1 and NTS2 receptors stably transfected into CHO or 1321N1 astrocytoma cells, respectively, according to the published procedures.⁹ Briefly, cells grown to confluence in 10 cm Petri dishes were frozen at –80 °C until use. On the day of the experiment, cells were submitted to a heat shock by placing the Petri dishes at 37 °C for 60 s before returning to ice. Cells were then harvested in ice-cold binding buffer (10 mM Tris buffer, 1 mM EDTA, pH 7.5) using a cell scraper and centrifuged at 3200g for 15 min at 4 °C. The pellet containing the membrane extract was resuspended in binding buffer. [¹²⁵I]-NT (with K_d (NTS1) = 0.7 nM and K_d (NTS2) = 3.4 nM) was used to determine the binding affinity of the test peptides (diluted in binding buffer supplemented with 50 mM Tris-HCl and 0.2% BSA, pH 7.5). Experiments were performed using 15–20 μ g of membrane proteins and 35,000 cpm, for CHO cell membranes expressing the hNTS1 receptors, or 200,000 cpm of the radiolabeled ligand for 1321N1 astrocytoma membranes expressing hNTS2 receptors. Incubations were performed for 60 min at ambient temperature, and the reaction was stopped by filtration using ice-cold binding buffer on filtered 96-well plates. Filters were placed in 5 mL tubes, and the radioactivity was determined using a WIZARD² automatic gamma counter (PerkinElmer, Canada). All experiments were performed in triplicate and repeated three times with independently prepared samples.

[³⁵S]GTP γ S Functional Assays for Opioid Receptors. Binding of [³⁵S]GTP γ S to membranes from CHO stably expressing the human opioid receptors was conducted according to the published procedures.²⁸ Cell membranes were prepared in buffer A (20 mM HEPES, 10 mM MgCl₂, and 100 mM NaCl, pH 7.4) as described for competitive radioligand binding assays. Cell membranes (5–10 μ g) in buffer A were incubated with 0.05 nM [³⁵S]GTP γ S, 10 μ M GDP, and various concentrations of test peptides in a final volume of 1 mL for 60 min at 25 °C. Nonspecific binding was determined using 10 μ M GTP γ S, and the basal binding was determined in the absence of the test ligand. Samples were filtered over Whatman glass GF/B fiber filters and counted as described for competitive binding assays. All experiments were performed in duplicate and repeated three times with independently prepared samples.

β -Arrestin-2 Recruitment Assay for the MOR. The measurement of hMOR-stimulated β -arrestin-2 recruitment was performed by the PathHunter β -arrestin-2 assay (DiscoverX, Birmingham, UK)

according to the published procedure.²⁵ U2OS cells stably coexpressing the human MOR and the enzyme acceptor (EA)-tagged β -arrestin-2 fusion protein (U2OS-hMOR- β -arrestin-2 cells) were seeded in the cell plating medium into 384-well white plates (Greiner Bio-One, Kremsmünster, Austria) at a density of 5000 cells in 20 μ L per well and maintained at 37 °C for 24 h. After incubation with various concentrations of test peptides in PBS for 90 min at 37 °C, the detection mix was added, and incubation was continued for additional 60 min at room temperature. Chemiluminescence was measured with the PHERAstar FSX plate reader (BMG LABTECH, Germany). All experiments were performed in duplicate and repeated three times with independently prepared samples.

BRET Assay for the NTS1 Receptor. A BRET-based *Gaq* activation assay was used to assess NTS1 receptor activation performed according to the published procedure.³⁵ The day before transfection, cultured HEK293 cells were washed with PBS at room temperature, trypsinized, and seeded at 3,500,000 cells in a 10 cm Petri dish. For transfection, 4 μ g of pcDNA3.1-3HA-hNTS1 with 800 ng of *Gaq*-RLucII,³⁶ 2.4 μ g of GFP10-Gy1, and 2.4 μ g of *G β 1*³⁷ were added to 600 μ L of 150 mM NaCl containing 36 μ g of PEI. The mixture was incubated for 15 min before being added to the cultured cells. At 24 h post-transfection, cells were washed with PBS, trypsinized, plated (75,000 cells/well) in 96-well white plates (BD Falcon, Corning, NY), and left for another 24 h. Cells were then equilibrated at room temperature for at least 30 min with 80 μ L of HBSS buffer. Coelenterazine 400A (an RLuc2 substrate) was added to a final concentration of 5 μ M. Cells were stimulated with the ligand ranging from 10 μ M to 1 pM and incubated for 10 min prior to the signal acquisition. BRET2 signals were measured using a GENios Pro plate reader (Tecan, Durham, NC, USA). RLuc2 and GFP10 emissions were collected in the 400–450 and 500–550 nm windows, respectively. The BRET2 signal was calculated as the ratio of light emitted by the acceptor GFP10 over the light emitted by the donor RLuc2. All experiments were performed in triplicate and repeated three times with independently prepared samples.

In Vivo Pharmacology. Animals and Drug Administration. Male CD-1 mice (30–35 g, 8 weeks old) were obtained from the Janvier Labs (Le Genest-Saint-Isle, France). Mice were group-housed in a temperature controlled room with a 12 h light/dark cycle and with free access to food and water. All animal studies were conducted in accordance with ethical guidelines and animal welfare standards according to Austrian regulations for animal research and were approved by the Committee of Animal Care of the Austrian Federal Ministry of Science and Research. Test peptides dissolved in saline or vehicle (saline) were administered by sc route in a volume of 10 μ L/1 g of body weight. Each experimental group included five to six animals. Separate groups of mice received the respective dose of peptide, and individual mice were only used once for behavioral testing.

Tail-Flick Test. The radiant heat tail-flick test was used to assess antinociceptive effects of test peptides after sc administration in mice using a UB 37360 Ugo Basile analgesimeter (Ugo Basile S.R.L., Varese, Italy), as described previously.^{18a} The reaction time required by the mouse to remove its tail after application of the radiant heat was measured and defined as the tail-flick latency (in seconds). Tail-flick latencies were measured before and after drug or saline sc administration (i.e., 15 min, 30 min, every hour up to 8 h, and 24 h). A cutoff time of 10 s was used in order to minimize tissue damage.

Data Analysis. Data were analyzed and graphically processed using GraphPad Prism software (GraphPad Prism Software Inc., San Diego, CA, USA) and are presented as means \pm SEM. The K_i (nM), potency EC_{50} (nM), and efficacy E_{max} (%) values were determined from concentration–response curves by nonlinear regression analysis. The K_i values were determined by the method of Cheng and Prusoff.³⁸ In the [³⁵S]GTP γ S binding assays, efficacy was determined relative to the reference full opioid agonists, DAMGO (MOR), DPDPE (DOR), and U69,593 (KOR). In the BRET assay, efficacy was determined relative to the reference NTS1 agonist NT(8-13). In the β -arrestin-2 recruitment assay, efficacy was determined relative to the reference MOR agonist DAMGO. In the tail-flick assay, the

antinociceptive effect (as percentage of maximum possible effect, % MPE) was calculated according to the formula = [(TL – BL)/(cutoff time – BL)] \times 100 where TL represents the test latency and BL is the basal latency. Data were statistically evaluated using two-way ANOVA with the Bonferroni post hoc test with significance set at $P < 0.05$.

In Vitro Human Plasma Stability. Human plasma stability assays were conducted and analyzed as published previously.¹¹ Human plasma was obtained from the Belgian Red Cross (Vlaams-Brabant, Leuven). Peptide 7 was dissolved in water (2 mM stock solution), and consecutive dilutions were prepared. A calibration curve was constructed (in triplicate), and the method was validated (linearity and precision). Stability experiments were performed in triplicate. After incubation of human plasma samples for at least 30 min, aqueous peptide solutions (1120 μ M) were spiked in human plasma (10:90 v/v peptide solution/plasma). Sampling was performed by taking 100 μ L of spiked plasma followed by the protein crash using 300 μ L of cold (4 °C) precipitation solvent (methanol containing 0.1% TFA v/v). The resulting suspensions were vortexed for 15 s and placed at 4 °C for 30 min. After centrifugation for 15 min, 100 μ L of supernatant was diluted with 100 μ L of water in the injection vial. Peptide half-life time was calculated based on the points with an area under the curve (AUC) higher than the AUC of the lowest standard concentration. Concentrations were calculated by the use of the calibration curve and transferred to a semi-log chart presenting the log concentrations as a function of time. Data analysis was performed using Microsoft Office 365 Excel.

■ ASSOCIATED CONTENT

Supporting Information

The Supporting Information is available free of charge at <https://pubs.acs.org/doi/10.1021/acs.jmedchem.0c01376>.

Analytical characterization (including HPLC and HRMS data) of the described analogues and competition binding curves from radioligand competition binding assays at the opioid and neurotensin receptors for the reference compounds KGOP01 and PK20 and new OP-NT hybrid peptide analogues 7 and 9 (PDF)

Molecular formula strings of the described analogues (CSV)

■ AUTHOR INFORMATION

Corresponding Authors

Philippe Sarret – Department of Pharmacology and Physiology, Faculty of Medicine and Health Sciences, Institut de Pharmacologie de Sherbrooke, Université de Sherbrooke, J1H 5N4 Sherbrooke, Canada; orcid.org/0000-0002-7627-701X; Email: philippe.sarret@usherbrooke.ca

Mariana Spetea – Department of Pharmaceutical Chemistry, Institute of Pharmacy and Center for Molecular Biosciences Innsbruck (CMBI), University of Innsbruck, 6020 Innsbruck, Austria; orcid.org/0000-0002-2379-5358; Email: mariana.spetea@uibk.ac.at

Steven Ballet – Research Group of Organic Chemistry, Departments of Chemistry and Bioengineering Sciences, Vrije Universiteit Brussel, 1050 Brussels, Belgium; orcid.org/0000-0003-4123-1641; Email: steven.ballet@vub.be

Authors

Simon Gonzalez – Research Group of Organic Chemistry, Departments of Chemistry and Bioengineering Sciences, Vrije Universiteit Brussel, 1050 Brussels, Belgium

Maria Dumitrascuta – Department of Pharmaceutical Chemistry, Institute of Pharmacy and Center for Molecular Biosciences Innsbruck (CMBI), University of Innsbruck, 6020 Innsbruck, Austria

Emilie Eiselt – Department of Pharmacology and Physiology, Faculty of Medicine and Health Sciences, Institut de Pharmacologie de Sherbrooke, Université de Sherbrooke, J1H 5N4 Sherbrooke, Canada

Stevany Louis – Department of Pharmaceutical Chemistry, Institute of Pharmacy and Center for Molecular Biosciences Innsbruck (CMBI), University of Innsbruck, 6020 Innsbruck, Austria

Linda Kunze – Department of Pharmaceutical Chemistry, Institute of Pharmacy and Center for Molecular Biosciences Innsbruck (CMBI), University of Innsbruck, 6020 Innsbruck, Austria

Annalisa Blasiol – Department of Pharmaceutical Chemistry, Institute of Pharmacy and Center for Molecular Biosciences Innsbruck (CMBI), University of Innsbruck, 6020 Innsbruck, Austria

Mélanie Vivancos – Department of Pharmacology and Physiology, Faculty of Medicine and Health Sciences, Institut de Pharmacologie de Sherbrooke, Université de Sherbrooke, J1H 5N4 Sherbrooke, Canada

Santo Previti – Research Group of Organic Chemistry, Departments of Chemistry and Bioengineering Sciences, Vrije Universiteit Brussel, 1050 Brussels, Belgium

Elke Dewolf – Research Group of Organic Chemistry, Departments of Chemistry and Bioengineering Sciences, Vrije Universiteit Brussel, 1050 Brussels, Belgium

Charlotte Martin – Research Group of Organic Chemistry, Departments of Chemistry and Bioengineering Sciences, Vrije Universiteit Brussel, 1050 Brussels, Belgium

Dirk Tourwé – Research Group of Organic Chemistry, Departments of Chemistry and Bioengineering Sciences, Vrije Universiteit Brussel, 1050 Brussels, Belgium

Florine Cavelier – Institut des Biomolécules Max Mousseron, UMR 5247, CNRS, Université de Montpellier, ENSCM, 34095 Montpellier, France; orcid.org/0000-0001-5308-6416

Louis Gendron – Department of Pharmacology and Physiology, Faculty of Medicine and Health Sciences, Institut de Pharmacologie de Sherbrooke, Université de Sherbrooke, J1H 5N4 Sherbrooke, Canada; orcid.org/0000-0002-2058-8863

Complete contact information is available at:
<https://pubs.acs.org/10.1021/acs.jmedchem.0c01376>

Notes

The authors declare no competing financial interest. [†]S.G., M.D., and E.E. contributed equally to this work. The manuscript was written through contributions of all authors. All authors have given approval to the final version of the manuscript.

ACKNOWLEDGMENTS

Drs. M. Bouvier, T. Hebert, S.A. Laporte, G. Pineyro, J.-C. Tardif, and E. Thorin (CQDM Team) are acknowledged for providing us with the Gαq biosensor. This work was supported by the Austrian Research Fund (FWF: I2463-B21 to M.S.), the Research Foundation Flanders (FWO Vlaanderen to S.B.), the Canadian Institutes of Health Research (CIHR) (FDN-148413 to P.S.), and the Natural Sciences and Engineering Research Council of Canada (NSERC) (RGPIN-2014-06358 to P.S.). P.S. holds a Canada Research Chair in Neurophysiopharmacology of Chronic Pain. E.E. was supported by a doctoral training award from the FRQ-S. M.D. was partly

supported by the University of Innsbruck PhD stipend program.

ABBREVIATIONS

(6-OH)Tic, 6-hydroxy-L-1,2,3,4-tetrahydroisoquinoline-3-carboxylic acid; Aba, 4-amino-1,2,4,5-tetrahydro-3H-benzo[c]-azepin-3-one; β³hArg, β³-homo arginine; β³hLys, β³-homo lysine; BBB, blood–brain barrier; BRET, bioluminescence resonance energy transfer; BSA, bovine serum albumin; CHO, Chinese hamster ovary; DCM, dichloromethane; DIC, N,N'-dicyclohexylcarbodiimide; DIPEA, diisopropylethylamine; DMF, N,N'-dimethylformamide; DMLs, designed multiple ligands; Dmt, 2',6'-dimethyltyrosine; DOR, δ-opioid receptor; EDTA, ethylenediaminetetraacetic acid; Fmoc, 9-fluorenylmethylloxycarbonyl; GPCRs, G protein-coupled receptors; HBTU, N,N,N',N'-tetramethyl-O-(1H-benzotriazol-1-yl)uronium hexafluorophosphate; HFIP, hexafluoroisopropanol; HOBt, 1-hydroxybenzotriazole; KOR, κ-opioid receptor; LC–MS, liquid chromatography–mass spectrometry; MOR, μ-opioid receptor; m-Tyr, meta-tyrosine; NMR, nuclear magnetic resonance; NPFF, neuropeptide FF; NT, neurotensin; NTS1, neurotensin 1 receptor; NTS2, neurotensin 2 receptor; OP, opioid; RP-HPLC, reversed-phase high-performance liquid chromatography; sc, subcutaneous; SPPS, solution phase peptide synthesis; TFA, trifluoroacetic acid; TIS, triisopropylsilane; Tle, tert-leucine

REFERENCES

- (1) Chou, R.; Turner, J. A.; Devine, E. B.; Hansen, R. N.; Sullivan, S. D.; Blazina, I.; Dana, T.; Bougatsos, C.; Deyo, R. A. The Effectiveness and Risks of Long-Term Opioid Therapy For Chronic Pain: A Systematic Review for a National Institutes of Health Pathways to Prevention Workshop. *Ann. Intern. Med.* **2015**, *162*, 276–286.
- (2) Coussens, N. P.; Sittampalam, G. S.; Jonson, S. G.; Hall, M. D.; Gorby, H. E.; Tamiz, A. P.; McManus, O. B.; Felder, C. C.; Rasmussen, K. The Opioid Crisis and the Future of Addiction and Pain Therapeutics. *J. Pharmacol. Exp. Ther.* **2019**, *371*, 396–408.
- (3) Pérez de Vega, M. J.; Ferrer-Montiel, A.; González-Muñiz, R. Recent Progress in Non-Opioid Analgesic Peptides. *Arch. Biochem. Biophys.* **2018**, *660*, 36–52.
- (4) Kleczkowska, P.; Lipkowski, A. W.; Tourwe, D.; Ballet, S. Hybrid Opioid/Non-Opioid Ligands in Pain Research. *Curr. Pharm. Des.* **2013**, *19*, 7435–7450.
- (5) (a) Turnaturi, R.; Chiechio, S.; Salerno, L.; Rescifina, A.; Pittalà, V.; Cantarella, G.; Tomarchio, E.; Parenti, C.; Pasquinucci, L. Progress in the Development of More Effective and Safer Analgesics for Pain Management. *Eur. J. Med. Chem.* **2019**, 111701. (b) Azzam, A. A. H.; McDonald, J.; Lambert, D. G. Hot Topics in Opioid Pharmacology: Mixed and Biased Opioids. *Br. J. Anaesth.* **2019**, *122*, e136–e145. (c) Grim, T. W.; Acevedo-Canabal, A.; Bohn, L. M. Toward Directing Opioid Receptor Signaling to Refine Opioid Therapeutics. *Biol. Psychiatry.* **2020**, *87*, 15–21.
- (6) Carraway, R.; Leeman, S. E. The Isolation of a New Hypotensive Peptide, Neurotensin, from Bovine Hypothalamus. *J. Biol. Chem.* **1973**, *248*, 6854–6861.
- (7) Sarret, P.; Cavelier, F., Neurotensin and its Receptors. In *Reference Module in Neuroscience and Biobehavioral Psychology*; Elsevier, Ed.: 2018; pp. 1–17.
- (8) Barroso, S.; Richard, F.; Nicolas-Ethève, D.; Reversat, J.-L.; Bernassau, J.-M.; Kitabgi, P.; Labbé-Jullié, C. Identification of Residues Involved in Neurotensin Binding and Modeling of the Agonist Binding Site in Neurotensin Receptor 1. *J. Biol. Chem.* **2000**, *275*, 328–336.
- (9) (a) Boules, M.; Liang, Y.; Briody, S.; Miura, T.; Fauq, I.; Oliveros, A.; Wilson, M.; Khaniyev, S.; Williams, K.; Li, Z.; Qi, Y.; Katovich, M.; Richelson, E. NT79: A Novel Neurotensin Analog with

- Selective Behavioral Effects. *Brain Res.* **2010**, *1308*, 35–46.
- (b) Demeule, M.; Beaudet, N.; Régina, A.; Besserer-Offroy, É.; Murza, A.; Tétrault, P.; Belleville, K.; Ché, C.; Larocque, A.; Thiot, C.; Béliveau, R.; Longpré, J.-M.; Marsault, É.; Leduc, R.; Lachowicz, J. E.; Gonias, S. L.; Castaigne, J.-P.; Sarret, P. Conjugation of a Brain-Penetrant Peptide with Neurotensin Provides Antinociceptive Properties. *J. Clin. Invest.* **2014**, *124*, 1199–1213. (c) Fanelli, R.; Besserer-Offroy, É.; René, A.; Côté, J.; Tétrault, P.; Collettere-Tremblay, J.; Longpré, J.-M.; Leduc, R.; Martinez, J.; Sarret, P.; Cavelier, F. Synthesis and Characterization in Vitro and in Vivo of (L)-(Trimethylsilyl)alanine Containing Neurotensin Analogues. *J. Med. Chem.* **2015**, *58*, 7785–7795. (d) Guillemette, A.; Dansereau, M. A.; Beaudet, N.; Richelson, E.; Sarret, P. Intrathecal Administration of NTS1 Agonists Reverses Nociceptive Behaviors in a Rat Model of Neuropathic Pain. *Eur. J. Pain* **2012**, *16*, 473–484. (e) Tétrault, P.; Beaudet, N.; Perron, A.; Belleville, K.; René, A.; Cavelier, F.; Martinez, J.; Stroh, T.; Jacobi, A. M.; Rose, S. D.; Behlke, M. A.; Sarret, P. Spinal NTS2 Receptor Activation Reverses Signs of Neuropathic Pain. *FASEB J.* **2013**, *27*, 3741–3752. (f) Dubuc, I.; Costentin, J.; Doulut, S.; Rodriguez, M.; Martinez, J.; Kitabgi, P. JMV 449: A Pseudopeptide Analogue of Neurotensin-(8–13) with Highly Potent and Long-Lasting Hypothermic and Analgesic Effects in the Mouse. *Eur. J. Pharmacol.* **1992**, *219*, 327–329.
- (10) (a) Al-Rodhan, N. R. F.; Richelson, E.; Gilbert, J. A.; McCormick, D. J.; Kanba, K. S.; Pfenning, M. A.; Nelson, A.; Larson, E. W.; Yaksh, T. L. Structure-Antinociceptive Activity of Neurotensin and Some Novel Analogues in the Periaqueductal Gray Region of the Brainstem. *Brain Res.* **1991**, *557*, 227–235. (b) Osbahr, A. J., 3rd; Nemeroff, C. B.; Luttinger, D.; Mason, G. A.; Prange, A. J., Jr. Neurotensin-Induced Antinociception in Mice: Antagonism by Thyrotropin-Releasing Hormone. *J. Pharmacol. Exp. Ther.* **1981**, *217*, 645–651. (c) Clineschmidt, B. V.; McGuffin, J. C.; Bunting, P. B. Neurotensin: Antinociceptive Action in Rodents. *Eur. J. Pharmacol.* **1979**, *54*, 129–139.
- (11) Eiselt, E.; Gonzalez, S.; Martin, C.; Chartier, M.; Betti, C.; Longpré, J.-M.; Cavelier, F.; Tourwé, D.; Gendron, L.; Ballet, S.; Sarret, P. Neurotensin Analogues Containing Cyclic Surrogates of Tyrosine at Position 11 Improve NTS2 Selectivity Leading to Analgesia without Hypotension and Hypothermia. *ACS Chem. Neurosci.* **2019**, *10*, 4535–4544.
- (12) (a) Morphy, R.; Rankovic, Z. Designed Multiple Ligands. An Emerging Drug Discovery Paradigm. *J. Med. Chem.* **2005**, *48*, 6523–6543. (b) Proschak, E.; Stark, H.; Merk, D. Polypharmacology by Design: A Medicinal Chemist's Perspective on Multitargeting Compounds. *J. Med. Chem.* **2019**, *62*, 420–444.
- (13) Drieu la Rochelle, A.; Guillemyn, K.; Dumitrascuta, M.; Martin, C.; Utard, V.; Quillet, R.; Schneider, S.; Daubeuf, F.; Willemse, T.; Mampuy, P.; Maes, B. U. W.; Frossard, N.; Bihel, F.; Spetea, M.; Simonin, F.; Ballet, S. A Bifunctional-Biased Mu-Opioid Agonist–Neuropeptide FF Receptor Antagonist as Analgesic with Improved Acute and Chronic Side Effects. *PAIN* **2018**, *159*, 1705–1718.
- (14) Boules, M.; Johnston, H.; Tozy, J.; Smith, K.; Li, Z.; Richelson, E. Analgesic Synergy of Neurotensin Receptor Subtype 2 Agonist NT79 and Morphine. *Behav. Pharmacol.* **2011**, *22*, 573–581.
- (15) Eiselt, E.; Côté, J.; Longpré, J.-M.; Blais, V.; Sarret, P.; Gendron, L. The Combination of Opioid and Neurotensin Receptor Agonists Improves their Analgesic/Adverse Effect Ratio. *Eur. J. Pharmacol.* **2019**, *848*, 80–87.
- (16) Kleczkowska, P.; Kosson, P.; Ballet, S.; Van den Eynde, I.; Tsuda, Y.; Tourwé, D.; Lipkowski, A. W. PK20, a New Opioid-Neurotensin Hybrid Peptide that Exhibits Central and Peripheral Antinociceptive Effects. *Mol. Pain* **2010**, *6*, 1744–8069.
- (17) Kleczkowska, P.; Hermans, E.; Kosson, P.; Kowalczyk, A.; Lesniak, A.; Pawlik, K.; Bojnik, E.; Benyhe, S.; Nowicka, B.; Bujalska-Zadrozny, M.; Misicka, A.; Lipkowski, A. W. Antinociceptive Effect Induced by a Combination of Opioid and Neurotensin Moieties vs. their Hybrid Peptide [Ile9]PK20 in an Acute Pain Treatment in Rodents. *Brain Res.* **2016**, *1648*, 172–180.
- (18) (a) Novoa, A.; Van Dorpe, S.; Wynendaele, E.; Spetea, M.; Bracke, N.; Stalmans, S.; Betti, C.; Chung, N. N.; Lemieux, C.; Zuegg, J.; Cooper, M. A.; Tourwé, D.; De Spiegeleer, B.; Schiller, P. W.; Ballet, S. Variation of the Net Charge, Lipophilicity, and Side Chain Flexibility in Dmt1-DALDA: Effect on Opioid Activity and Biodistribution. *J. Med. Chem.* **2012**, *55*, 9549–9561. (b) Guillemyn, K.; Kleczkowska, P.; Lesniak, A.; Dyniewicz, J.; Van der Poorten, O.; Van den Eynde, I.; Keresztes, A.; Varga, E.; Lai, J.; Porreca, F.; Chung, N. N.; Lemieux, C.; Mika, J.; Rojewski, E.; Makuch, W.; Van Duppen, J.; Przewlocka, B.; Vanden Broeck, J.; Lipkowski, A. W.; Schiller, P. W.; Tourwé, D.; Ballet, S. Synthesis and Biological Evaluation of Compact, Conformationally Constrained Bifunctional Opioid Agonist – Neurokinin-1 Antagonist Peptidomimetics. *Eur. J. Med. Chem.* **2015**, *92*, 64–77. (c) Dumitrascuta, M.; Bermudez, M.; Ballet, S.; Wolber, G.; Spetea, M. Mechanistic Understanding of Peptide Analogues, DALDA, [Dmt¹]DALDA, and KGOP01, Binding to the Mu Opioid Receptor. *Molecules* **2020**, *25*, 2087.
- (19) (a) Guillemyn, K.; Starnowska, J.; Lagard, C.; Dyniewicz, J.; Rojewski, E.; Mika, J.; Chung, N. N.; Utard, V.; Kosson, P.; Lipkowski, A. W.; Chevillard, L.; Arranz-Gibert, P.; Teixidó, M.; Megarbane, B.; Tourwé, D.; Simonin, F.; Przewlocka, B.; Schiller, P. W.; Ballet, S. Bifunctional Peptide-Based Opioid Agonist–Nociceptin Antagonist Ligands for Dual Treatment of Acute and Neuropathic Pain. *J. Med. Chem.* **2016**, *59*, 3777–3792. (b) Lagard, C.; Chevillard, L.; Guillemyn, K.; Risède, P.; Laplanche, J.-L.; Spetea, M.; Ballet, S.; Mégarbane, B. Bifunctional Peptide-Based Opioid Agonist/Nociceptin Antagonist Ligand for Dual Treatment of Nociceptive and Neuropathic Pain. *Pain* **2017**, *158*, 505–515.
- (20) (a) Bredeloux, P.; Cavelier, F.; Dubuc, I.; Vivet, B.; Costentin, J.; Martinez, J. Synthesis and Biological Effects of c(Lys-Lys-Pro-Tyr-Ile-Leu-Lys-Lys-Pro-Tyr-Ile-Leu) (JMV2012), a New Analogue of Neurotensin that Crosses the Blood–Brain Barrier. *J. Med. Chem.* **2008**, *51*, 1610–1616. (b) Hapău, D.; Rémond, E.; Fanelli, R.; Vivancos, M.; René, A.; Côté, J.; Besserer-Offroy, É.; Longpré, J.-M.; Martinez, J.; Zaharia, V.; Sarret, P.; Cavelier, F. Stereoselective Synthesis of β -(5-Arylthiazolyl) α -Amino Acids and Use in Neurotensin Analogues. *Eur. J. Org. Chem.* **2016**, *2016*, 1017–1024.
- (21) (a) Tyler, B. M.; Douglas, C. L.; Fauq, A.; Pang, Y.-P.; Stewart, J. A.; Cusack, B.; McCormick, D. J.; Richelson, E. In Vitro Binding and CNS Effects of Novel Neurotensin Agonists that Cross the Blood–Brain Barrier. *Neuropharmacology* **1999**, *38*, 1027–1034. (b) Kokko, K. P.; Hadden, M. K.; Orwig, K. S.; Mazella, J.; Dix, T. A. In Vitro Analysis of Stable, Receptor-Selective Neurotensin[8–13] Analogues. *J. Med. Chem.* **2003**, *46*, 4141–4148. (c) Schindler, L.; Bernhardt, G.; Keller, M. Modifications at Arg and Ile Give Neurotensin(8–13) Derivatives with High Stability and Retained NTS₁ Receptor Affinity. *ACS Med. Chem. Lett.* **2019**, *10*, 960–965.
- (22) (a) Richard, F.; Barroso, S.; Martinez, J.; Labbé-Jullié, C.; Kitabgi, P. Agonism, Inverse Agonism, and Neutral Antagonism at the Constitutively Active Human Neurotensin Receptor 2. *Mol. Pharmacol.* **2001**, *60*, 1392–1398. (b) Held, C.; Plomer, M.; Hübner, H.; Meltretter, J.; Pischetsrieder, M.; Gmeiner, P. Development of a Metabolically Stable Neurotensin Receptor 2 (NTS₂) Ligand. *ChemMedChem* **2013**, *8*, 75–81. (c) Heyl, D. L.; Seifler, N. M.; He, J. X.; Sawyer, T. K.; Wustrow, D. J.; Akunne, H. C.; Davis, M. D.; Pugsley, T. A.; Heffner, T. G.; Corbin, A. E.; Cody, W. L. Structure-Activity and Conformational Studies of a Series of Modified C-terminal Hexapeptide Neurotensin Analogues. *Int. J. Pept. Protein Res.* **1994**, *44*, 233–238. (d) Fanelli, R.; Floquet, N.; Besserer-Offroy, É.; Delort, B.; Vivancos, M.; Longpré, J.-M.; Renault, P.; Martinez, J.; Sarret, P.; Cavelier, F. Use of Molecular Modeling to Design Selective NTS₂ Neurotensin Analogues. *J. Med. Chem.* **2017**, *60*, 3303–3313.
- (23) (a) Couder, J.; Tourwé, D.; Binst, G.; Schuurkens, J.; Leysen, J. E. Synthesis and Biological Activities of ψ (CH₂NH) Pseudopeptide Analogues of the C-terminal Hexapeptide of Neurotensin. *Int. J. Pept. Protein Res.* **1993**, *41*, 181–184. (b) Einsiedel, J.; Hübner, H.; Hervet, M.; Härterich, S.; Koschatzky, S.; Gmeiner, P. Peptide Backbone Modifications on the C-terminal Hexapeptide of Neurotensin. *Bioorg. Med. Chem. Lett.* **2008**, *18*, 2013–2018. (c) Lugin, D.; Vecchini, F.;

Doulut, S.; Rodriguez, M.; Martinez, J.; Kitabgi, P. Reduced Peptide Bond Pseudopeptide Analogues of Neurotensins Binding and Biological Activities, and In Vitro Metabolic Stability. *Eur. J. Pharmacol.* **1991**, *205*, 191–198.

(24) Chan, W.; White, P. *Fmoc Solid Phase Peptide Synthesis a Practical Approach*; Oxford University Press: Oxford, 2000.

(25) Martin, C.; Dumitrascuta, M.; Mannes, M.; Lantero, A.; Bucher, D.; Walker, K.; Van Wanseele, Y.; Oyen, E.; Hernot, S.; Van Eeckhaut, A.; Madder, A.; Hoogenboom, R.; Spetea, M.; Ballet, S. Biodegradable Amphipathic Peptide Hydrogels as Extended-Release System for Opioid Peptides. *J. Med. Chem.* **2018**, *61*, 9784–9789.

(26) Kleczkowska, P.; Bojnik, E.; Leśniak, A.; Kosson, P.; Eynde, I. V. d.; Ballet, S.; Benyhe, S.; Tourwé, D.; Lipkowski, A. W. Identification of Dmt-D-Lys-Phe-Phe-OH as a Highly Antinociceptive Tetrapeptide Metabolite of the Opioid-Neurotensin Hybrid Peptide PK20. *Pharmacol. Rep.* **2013**, *65*, 836–846.

(27) White, J. F.; Noinaj, N.; Shibata, Y.; Love, J.; Kloss, B.; Xu, F.; Gvozdenovic-Jeremic, J.; Shah, P.; Shiloach, J.; Tate, C. G.; Grisshammer, R. Structure of the Agonist-Bound Neurotensin Receptor. *Nature* **2012**, *490*, 508–513.

(28) Spetea, M.; Rief, S. B.; Haddou, T. B.; Fink, M.; Kristeva, E.; Mittendorfer, H.; Haas, S.; Hummer, N.; Follia, V.; Guerrieri, E.; Asim, M. F.; Sturm, S.; Schmidhammer, H. Synthesis, Biological, and Structural Explorations of New Zwitterionic Derivatives of 14-O-Methylxymorphone, as Potent μ/δ Opioid Agonists and Peripherally Selective Antinociceptives. *J. Med. Chem.* **2019**, *62*, 641–653.

(29) Mores, K. L.; Cummins, B. R.; Cassell, R. J.; van Rijn, R. M. A Review of the Therapeutic Potential of Recently Developed G Protein-Biased Kappa Agonists. *Front. Pharmacol.* **2019**, *10*, 407.

(30) Violin, J. D.; Crombie, A. L.; Soergel, D. G.; Lark, M. W. Biased Ligands at G-Protein-Coupled Receptors: Promise and Progress. *Trends Pharmacol. Sci.* **2014**, *35*, 308–316.

(31) Besserer-Offroy, É.; Brouillette, R. L.; Lavenus, S.; Froehlich, U.; Brumwell, A.; Murza, A.; Longpré, J.-M.; Marsault, É.; Grandbois, M.; Sarret, P.; Leduc, R. The Signaling Signature of the Neurotensin Type 1 Receptor with Endogenous Ligands. *Eur. J. Pharmacol.* **2017**, *805*, 1–13.

(32) (a) Thomas, J. B.; Giddings, A. M.; Wiethe, R. W.; Olepu, S.; Warner, K. R.; Sarret, P.; Gendron, L.; Longpre, J.-M.; Zhang, Y.; Runyon, S. P.; Gilmour, B. P. Identification of 1-({[1-(4-Fluorophenyl)-5-(2-methoxyphenyl)-1H-pyrazol-3-yl]carbonyl}-amino)cyclohexane Carboxylic Acid as a Selective Nonpeptide Neurotensin Receptor Type 2 Compound. *J. Med. Chem.* **2014**, *57*, 5318–5332. (b) Thomas, J. B.; Vivancos, M.; Giddings, A. M.; Wiethe, R. W.; Warner, K. R.; Murza, A.; Besserer-Offroy, É.; Longpré, J.-M.; Runyon, S. P.; Decker, A. M.; Gilmour, B. P.; Sarret, P. Identification of 2-({[1-(4-Fluorophenyl)-5-(2-methoxyphenyl)-1H-pyrazol-3-yl]carbonyl}amino)tricyclo[3.3.1.1^{3,7}]decane-2-carboxylic Acid (NTRC-844) as a Selective Antagonist for the Rat Neurotensin Receptor Type 2. *ACS Chem. Neurosci.* **2016**, *7*, 1225–1231.

(33) (a) Roussy, G.; Dansereau, M.-A.; Doré-Savard, L.; Belleville, K.; Beaudet, N.; Richelson, E.; Sarret, P. Spinal NTS1 Receptors Regulate Nociceptive Signaling in a Rat Formalin Tonic Pain Model. *J. Neurochem.* **2008**, *105*, 1100–1114. (b) Lafrance, M.; Roussy, G.; Belleville, K.; Maeno, H.; Beaudet, N.; Wada, K.; Sarret, P. Involvement of NTS2 Receptors in Stress-Induced Analgesia. *Neuroscience* **2010**, *166*, 639–652.

(34) Tourwé, D.; Iterbeke, K.; Kazmierski, W. M.; Tóth, G. Cyclic Aromatic Amino Acids with Constrained χ_1 and χ_2 Dihedral Angles. In *Peptidomimetics Protocols*; Kazmierski, W. M., Ed. Humana Press: Totowa, NJ, 1999; pp. 321–338.

(35) Sousbie, M.; Vivancos, M.; Brouillette, R. L.; Besserer-Offroy, É.; Longpré, J.-M.; Leduc, R.; Sarret, P.; Marsault, É. Structural Optimization and Characterization of Potent Analgesic Macrocyclic Analogues of Neurotensin (8–13). *J. Med. Chem.* **2018**, *61*, 7103–7115.

(36) Breton, B.; Sauvageau, É.; Zhou, J.; Bonin, H.; Le Guill, C.; Bouvier, M. Multiplexing of Multicolor Bioluminescence Resonance Energy Transfer. *Biophys. J.* **2010**, *99*, 4037–4046.

(37) Galés, C.; Van Durm, J. J. J.; Schaak, S.; Pontier, S.; Percherancier, Y.; Audet, M.; Paris, H.; Bouvier, M. Probing the Activation-Promoted Structural Rearrangements in Preassembled Receptor–G Protein Complexes. *Nat. Struct. Mol. Biol.* **2006**, *13*, 778–786.

(38) Cheng, Y. C.; Prusoff, W. H. Relationship Between the Inhibition Constant (KI) and the Concentration of Inhibitor which Causes 50 Per Cent Inhibition (I50) of an Enzymatic Reaction. *Biochem. Pharmacol.* **1973**, *22*, 3099–3108.